It should be pointed out here that the gain-bandwidth relations obtained here are not optimal in the sense of the ideal bandpass lumped domain response [8]. They are optimum for the case of the ideal periodic passband obtained using the $\Omega = \tan \theta$ transformation. Therefore, the results are valid for the comparison of an actual nth-order structure having periodic passbands with the ideal case.

VI. Conclusions

The gain-bandwidth relations for single-stub transmission-line structures have been investigated. The results are explicit for $n = 1$ for both Chebyshev and Butterworth approximations. The results for $n = 1$ and $n = 2$ are compared with the optimal reactance absorption curve for the ideal-gain response. As we decrease K or increase ε reactance absorption increases and the amount of the tradeoff involved is easily obtained from either the graphs or the tables.

The results of Carlin and Kohler [2] for resistor ratio adjustment for gain factor $K = 1$ have been extended for $0 < K \leq 1$. The results are also related for the reactance absorption properties of this type of structure.

Acknowledgment

The authors wish to thank Prof. H. J. Carlin of Cornell University for many helpful discussions and suggestions.

References

[1] E. M. T. Jones, "Synthesis of wide-band microwave filters to have prescribed insertion loss," *1956 IRE Convention Record*, pt. V, pp. 119–126.
[2] H. J. Carlin and W. Kohler, "Direct synthesis of band-pass transmission line structures," *IEEE Trans. Microwave Theory Tech.*, vol. MTT-13, May 1965.
[3] H. J. Carlin, "Distributed circuit design with transmission-line elements," *Proc. IEEE*, vol. 59, July 1971.
[4] G. Hoffman and H. Vanooteghem, "DISFIL, a computer program for optimum synthesis of TEM transmission-line filters," *IEEE Trans. Microwave Theory Tech.*, vol. MTT-20, p. 709, Oct. 1972.
[5] G. L. Matthaei, L. Young, and E. M. T. Jones, *Microwave Filters, Impedance Matching Networks, and Coupling Structures.* New York: McGraw-Hill, 1964.
[6] R. M. Fano, "Theoretical limitations on the broad-band matching of arbitrary impedances," *J. Franklin Institute*, vol. 249, pp. 57–83, Jan. 1950, also pp. 139–154, Feb. 1950.
[7] D. C. Youla, "A new theory of broad-band matching," *IEEE Trans. Circuit Theory*, vol. CT-11, pp. 30–50, Mar. 1964.
[8] H. J. Carlin and R. A. Friedenson, "Gain bandwidth properties of a distributed parameter load," *IEEE Trans. Circuit Theory*, vol. CT-15, pp. 455–464, Dec. 1968.

Letters

Noise Calibration Repeatability of an Airborne Third-Generation Radiometer

HANS-JUERGEN C. BLUME

Abstract—**A third-generation S-band radiometer has been calibrated at intervals over $3\frac{1}{2}$ years. The built-in stabilization concepts have proven to be very effective. In spite of some nonideal conditions (on runway, in wind, and in rain), an rms value of 0.7 K calibration repeatability has been observed with an average temperature deviation (bias error) of 0.03 K.**

Introduction

This third-generation radiometer is a 2.65-GHz (S-band) apparatus [1], which has been operated during about $3\frac{1}{2}$ years for about 400 h from aircraft or other elevated platforms. At intervals, the radiometer has been calibrated with a cryogenic noise source positioned in front of the antenna aperture. The measurement deviation from the temperature of the calibrated noise source represents an indication of the longtime stability of the overall characteristic of the radiometer. These deviations are presented and discussed for the $3\frac{1}{2}$ years of existence of the radiometer.

Manuscript received May 10, 1976; revised April 11, 1977.
The author is with NASA Langley Research Center, Hampton, VA 23665.

Calibration Procedures

A schematic representation of the calibration setup and the operation during calibration is shown in Fig. 1 in the form of a block diagram. As can be seen in Fig. 1 two concepts have been added to the first-generation Dicke radiometer [2]. The first concept consists in equalizing the temperature of the reference noise source at the second input of the Dicke switch with the temperature of the lossy microwave components between the antenna terminal and receiver input; once these temperatures are equalized they are kept extremely constant (± 0.03 K). The second concept consists in injecting pulsed portions from a constant noise source of higher noise power (avalanche diode) into the received noise power until the noise power of both Dicke-switch inputs is the same. The pulse frequency which determines the average value of the injected noise power is controlled by a feedback system. The pulse frequency is then a measure of the noise power (radiation) received by the antenna. In addition to eliminating both the time-consuming calibration cycles of the second-generation radiometer [3] and the noise effects of the microwave components, these two concepts also have the advantage of establishing longtime stability of the overall characteristic of the radiometer, in spite of gain variations, changes of losses, and other aging effects, as long as the noise source output power for noise injection remains constant. The ambient temperature of the noise source is stabilized to $\pm 1°$ C.

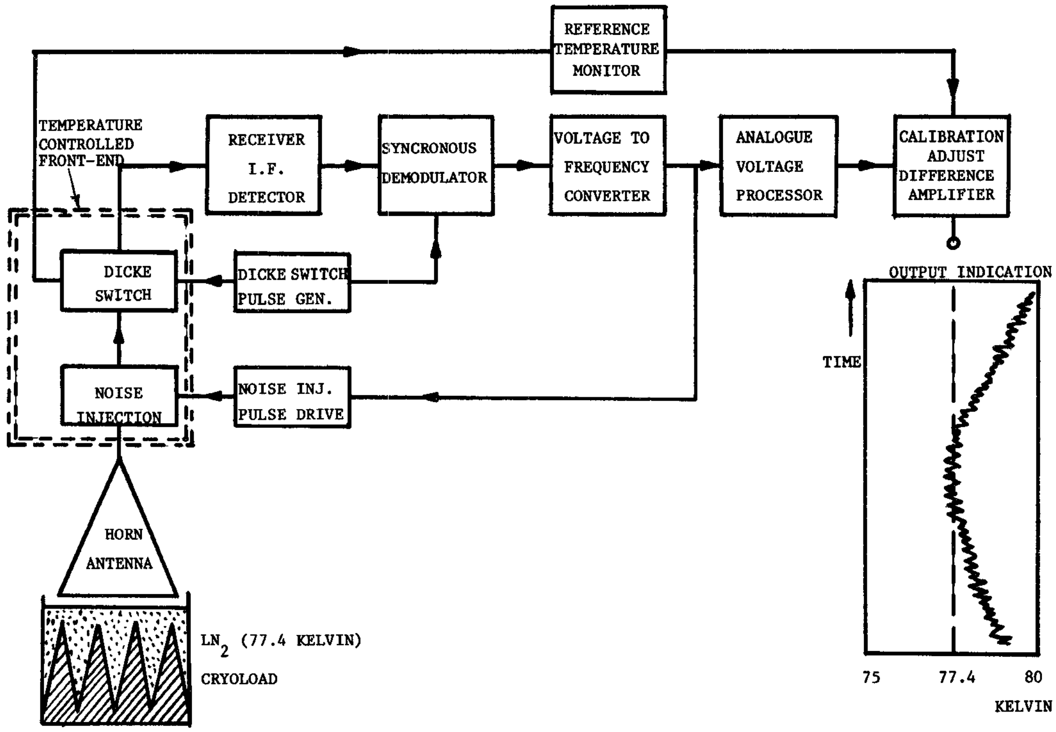

Fig. 1 Block diagram of the S-band radiometer calibration setup.

Calibration of the S-band radiometer is accommodated by placing a matched load of known temperature over the entire aperture of the receiving horn antenna. This source is a box containing microwave absorbing material with pyramidical absorption facets that are cooled with liquid nitrogen as described in [4]. The reflection coefficient at the top of the matched load was 10^{-4}, requiring only a negligible correction of 0.02 K. After reaching the equilibrium temperature, the calibration noise source is lifted under the aircraft against the aperture of the antenna. Aluminized Mylar flaps are fastened to the outside of the antenna in order to prevent interference from extraneous noise sources, such as radiation from the aircraft fuselage or from the relatively "hot" ground. If calibration is done in a hangar, light sources such as gas discharge lamps may act as a strong interfering source; therefore, the shielding with the aluminized Mylar must be tight. After positioning the calibration source under the antenna aperture, liquid nitrogen is resupplied so that the liquid level is just above the styrofoam that surrounds the pyramidical absorbers. Since the relative dielectric constant of liquid nitrogen is 1.4, a discontinuity initially exists between the antenna and absorbing material, and causes a high (2 K) radiometer indication. During the evaporation of the excess liquid, this error becomes smaller and reaches zero as soon as only the pyramids themselves are filled with the cryogen. At this time the indication reaches a minimum. During further evaporation, the pyramid peaks warm up and the indication increases again. If the calibration is attempted to a precision of 0.1 K, the output minimum must be determined very carefully with a longtime (10-min) averaging process. If the minimum of the temperature indication deviated from the calibration temperature (liquid nitrogen), the indicated value was recorded and the radiometer recalibrated with the calibration adjustment (see Fig. 1).

Since the reference load at the Dicke switch and the front-end losses of this type of radiometer are at the same fixed, stable temperature, a second calibration with a source at a different calibration temperature, as for second-generation radiometers, is not required.

Accuracy Considerations

The boiling point of liquid nitrogen (in kelvins) varies with atmospheric pressure according to the following equation:

$$T = 77.36 - 0.011(760 - p) \tag{1}$$

where p is the atmospheric pressure in millimeters of mercury. Each calibration therefore requires a correction for atmospheric pressure.

The physical temperature also affects the calibration because the antenna is not completely loss free and cannot be temperature stabilized as thoroughly as can the front-end microwave components. To estimate this loss contribution, we use [3, p. 385, equation 13]:

$$\Delta = \frac{l}{1 - l - R}\left[(T_0 - T_p) - \frac{f}{f_c}(T_0 - T_{pc})\right].$$

It may be assumed that from one calibration to the next, the frequency ratio in (13) is very close to unity. We obtain, with a slight change in notation,

$$\Delta = \frac{l}{1 - l - R}(T_n - T_{n-1}) \tag{2}$$

where T_n is the physical temperature of the antenna during the calibration in question and T_{n-1} is the temperature of the antenna during the preceding calibration. The sum of the antenna losses l is 0.025 and the reflection losses R are negligible for the S-band radiometer. After applying these values and adding (2) to (1), we obtain the following:

$$T_c = 77.36 + 0.011(p - 760) + 0.025(T_n - T_{n-1}) \tag{3}$$

TABLE I
S-BAND RADIOMETER CALIBRATION RECORD

CAL. NO.	DATE	PHYSICAL ANTENNA TEMP. (K)	CORR. 0.025 x (T_N-T_{N-1}) (K)	BAROM. PRESSURE (MM HG)	CORR. 0.011 x (P-760) (K)	CAL. TEMP. T_C (K)	MEAS. TEMP. T_{IND} (K)	ΔT_C = (T_C-T_{IND}) (K)
1	05-15-72	296	0	758.2	- 0.02	77.34		
2	05-24-72	291	- 0.12	757.9	- 0.02	77.22	77.45	- 0.23
3	06-13-72	296	+ 0.12	762.0	+ 0.02	77.5	76.36	+ 1.14
4	06-14-72	296	0	762.0	+ 0.02	77.38	77.44	- 0.06
5	07-11-72	301	+ 0.13	762.0	+ 0.02	77.51	77.84	- 0.33
6	07-17-72	302	+ 0.02	764.5	+ 0.05	77.43	77.76	- 0.33
7	07-19-72	301	- 0.02	765.6	+ 0.06	77.4	76.7	+ 0.7
8	10-13-72	295	- 0.15	764.0	+ 0.05	77.26	76.9	+ 0.36
9	10-16-72	301	- 0.15	764.5	+ 0.05	77.56	79.2	- 1.64
10	10-18-72	289	- 0.3	767.9	+ 0.09	77.15	77.4	- 0.25
11	10-24-72	293	+ 0.1	759.5	- 0.01	77.45	76.6	+ 0.85
12	10-27-72	290	- 0.18	766.3	+ 0.07	77.25	77.84	- 0.59
13	11-16-72	287	- 0.07	765.1	+ 0.06	77.35	78.1	- 0.75
14	12-04-72	294	+ 0.17	765.9	+ 0.07	77.6	77.0	+ 0.6
15	12-06-72	293	- 0.02	762.0	+ 0.02	77.36	77.2	+ 0.16
16	12-08-72	291	- 0.05	769.1	+ 0.1	77.41	77.26	+ 0.15
17	03-01-73	292	+ 0.02	772.4	+ 0.14	77.52	76.7	+ 0.82
18	08-29-73	302	+ 0.25	763.8	+ 0.05	77.66	77.6	+ 0.06
19	09-24-73	289	- 0.33	763.0	+ 0.03	77.06	78.6	- 1.54
20	09-27-73	285	- 0.1	762.0	+ 0.02	77.28	77.45	- 0.17
21	07-25-74	302	+ 0.42	764.3	+ 0.05	77.83	77.2	+ 0.63
22	07-31-74	318	+ 0.4	762.0	+ 0.02	77.78	77.75	- 0.03
23	01-17-75	291	- 0.68	777.2	+ 0.19	76.87	77.4	- 0.53
24	03-18-75	296	+ 0.12	777.2	+ 0.19	77.67	77.2	+ 0.47
25	08-05-75	301	+ 0.13	762.0	+ 0.02	77.51	76.62	+ 0.89
26	08-19-75	297	- 0.1	762.0	+ 0.02	77.28	76.95	+ 0.33

where T_c in kelvins is the calibration temperature that the radiometer would indicate if the overall characteristic of the radiometer did not change at all from calibration to calibration. In order to characterize the stability of the radiometer, we use the difference ΔT_c between the calibration temperature T_c and the indicated temperature T_{ind}, which is a measure of the change from the previous calibration:

$$\Delta T_c = T_c - T_{\text{ind}}. \tag{4}$$

Table I, entitled "*S*-band Radiometer Calibration Record," shows 26 calibrations that are distributed over $3\frac{1}{2}$ years. The third and fourth columns of the table indicate the physical temperature of the antenna and the corresponding correction. The first physical temperature, 296 K, is used as the base or starting temperature. The correction from one calibration to the next may be more than 1 K if the physical temperature of the antenna changes drastically.

Atmospheric pressure variations, as they are indicated in column 5, result in smaller corrections up to 0.2 K. The last three columns show the three terms of (4). The values of the last column are presented in Fig. 2 as a histogram of the 26 calibrations. The first calibration is used as the reference point. The maximal deviations amount to 1.6 K. The average temperature deviation is 0.03 K and the rms value is 0.7 K. This 0.7 K rms value represents only the system calibration repeatability and indicates nothing about the absolute measurement accuracy and brightness temperature resolution.

The smallest effects during calibration, such as formation of ice above the absorbing pyramids, subjective judgment in finding the indication minimum, and slight vertical motions of the aircraft fuselage (also the antenna aperture) in reference to the calibration source, may offset the attempted precision of 0.1 K by 0.5 K. In this respect, the stability of the tested *S*-band radiometer may be better than indicated. Because of the long term stability of this instrument, very frequent calibrations would not be necessary if calibration measurements were conducted under the following optimal conditions:

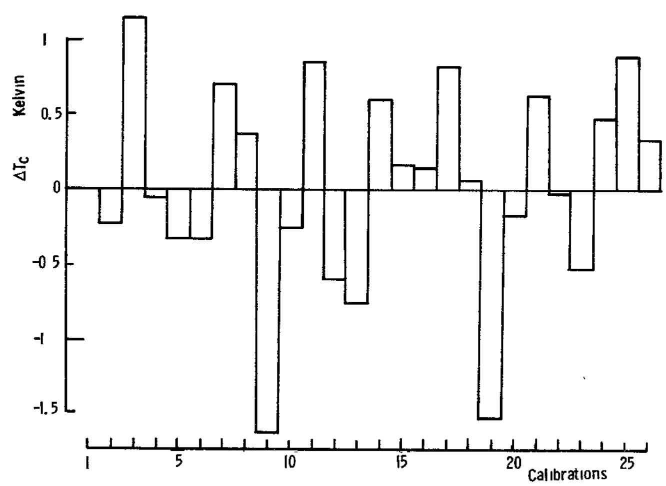

Fig. 2 $3\frac{1}{2}$ year calibration histogram of the *S*-band radiometer.

a) in the hangar protected from weather;
b) low humidity;
c) no wind gusts;
d) no perturbation of the tight seal of Mylar flaps (motionless aircraft).

CONCLUDING REMARKS

An *S*-band radiometer of the third generation has been tested and calibrated over a time interval of $3\frac{1}{2}$ years. The stabilization concepts which have been built into the radiometer have been proved so effective that changes in the radiometer cannot be distinguished from possible calibration inaccuracies. Over this $3\frac{1}{2}$ years maximum calibration deviations of 1.6 K and rms variations of 0.7 K have been observed. However, it must be pointed out that conditions during some calibrations were not ideal, and inaccuracies may have occurred which, in turn, caused a fictitious instability of the radiometer. Therefore, it is advantageous to recalibrate the instrument only when the climatic effects are small and sufficient time is available for a thorough and careful calibration procedure.

References

[1] W. N. Hardy, K W Gray, and A W. Love, "An S-band radiometer design with high absolute precision," *IEEE Trans Microwave Theory Tech.*, vol. MTT-22, pp. 382–390, Apr 1974

[2] R. H. Dicke, "The measurement of thermal radiation at microwave frequencies," *Review of Scientific Instruments*, vol. 17, pp. 268–275, July 1946

[3] M E. Tiuri, "Radio astronomy receivers," *IEEE Trans. Antennas Propagat*, vol. AP-12, pp 930–938, Dec. 1964.

[4] W. N Hardy, "Precision temperature reference for microwave radiometry," *IEEE Trans. Microwave Theory Tech*, vol MTT-21, pp. 149–150, Mar. 1973.

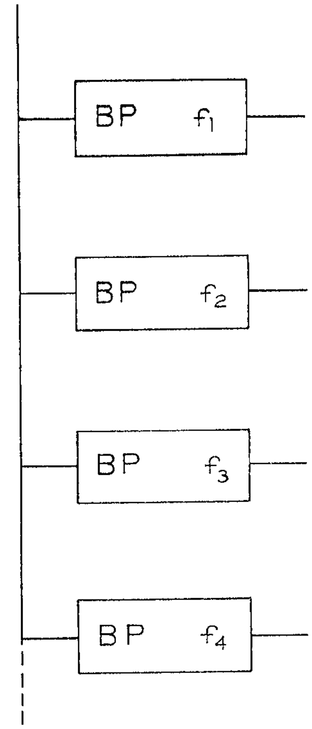

Fig 1. Multicoupler block diagram.

Resonant Cavities Used as Frequency Selective Phase Shifters

N. A. McDONALD

Abstract—**An application of resonant cavities as frequency selective phase shifters in a multicoupler configuration is described.**

When several bandpass filters are to be sequentially branched off a transmission line to form a multicoupler as in Fig. 1, some method has to be used to obtain, at the pass frequency of each bandpass filter, the correct impedance (usually an open circuit) immediately below the junction of that bandpass filter and the main transmission line.

Two common ways to achieve this are:

a) to insert below each bandpass filter a bandstop filter tuned to the same frequency;
b) to insert below each bandpass filter an adjustable phase shifter, and to terminate the main transmission line beyond the last bandpass filter in a short circuit or reactance.

This letter relates to an alternative configuration in which resonant cavities are used as frequency selective phase shifters beyond the last bandpass filter.

Consider the network of Fig. 2, in which all of the series resonant circuits are of high Q and independently tunable, and in which each series circuit presents a high impedance at the junction T except in the vicinity of the resonant frequency of that circuit. If a signal at fixed frequency f_1 is applied to the transmission line above T and one of the series circuits is tuned through resonance at f_1, the admittance that the series circuit presents at the junction T, in principle, passes through all reactive values. Accordingly the standing wave pattern at f_1 on the transmission line above T moves a distance of one-half wavelength and is therefore capable of presenting any reactive impedance at any point on the line above T.

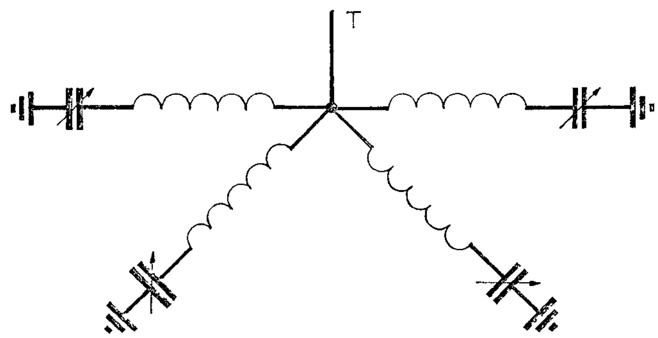

Fig. 2. Parallel combination of resonators

Such a combination of resonant circuits acts as a frequency selective phase shifter having as many independently adjustable phase/frequency combinations as there are resonant circuits. If such a network is placed below the lowest filter in Fig. 1, the necessary impedance requirements can be met at the junctions between bandpass filters and the main transmission line. Although in principle the stopband impedances of the bandpass filters at the main transmission line are infinite, any residual reactances can be absorbed in the phase shift adjustment.

Manuscript received March 25, 1977.

The author was with Antenna Engineering Australia Pty. Ltd., Kilsyth 3137, Australia. He is now with the Royal Melbourne Institute of Technology, Melbourne, Victoria 3001, Australia.